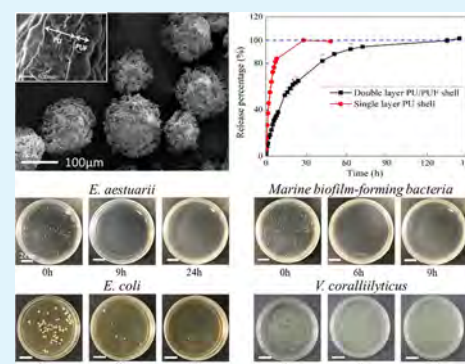


Fabrication and Release Behavior of Microcapsules with Double-Layered Shell Containing Clove Oil for Antibacterial Applications

Yong-Bing Chong,[†] He Zhang,[‡] Chee Yoon Yue,^{*,†} and Jinglei Yang^{*,§}[†]School of Mechanical and Aerospace Engineering, Nanyang Technological University, 50 Nanyang Avenue, Singapore 639798, Singapore[‡]South China University of Technology, National Engineering Research Center of Novel Equipment for Polymer Processing, Ministry of Education, Key Laboratory Polymer Processing Engineering, Guangzhou 510641, China[§]Department of Mechanical and Aerospace Engineering, The Hong Kong University of Science and Technology, Clear Water Bay, Kowloon, Hong Kong SAR, China

ABSTRACT: In this study, double-layer polyurethane/poly(urea-formaldehyde) (PU/PUF) shell microcapsules containing clove oil with antibacterial properties were successfully synthesized via in situ and interfacial polymerization reactions in an oil-in-water emulsion. The morphology, core-shell structure, and composition of the microcapsules were investigated systematically. Additionally, the release behaviors of microcapsules synthesized under different reaction parameters were studied. It was found that the release rate of clove oil can be controlled by tuning the amount of PU reactants and the length of PUF deposition time. The release profile fitted well against the Baker–Lonsdale model, which indicates diffusion as the primary release mechanism. Experimental results based on the ASTM E2315 time kill test revealed that the fabricated microcapsules have great antibacterial activities against the marine bacteria *Vibrio coralliilyticus*, *Escherichia coli*, *Exiguobacterium aestuarii*, and marine biofilm-forming bacteria isolated from the on-site contaminated samples, showing their great potential as an eco-friendly solution to replace existing toxic antifouling agent.

KEYWORDS: antifouling, clove oil, controlled release, antibacterial, microencapsulation



INTRODUCTION

Biofouling is defined as the settlement of marine organisms onto any surface immersed in seawater. Several adverse effects of biofouling include increased drag reduction of ship and increased fuel consumption,¹ which had caused huge economic losses annually, especially for the marine industry. Thus, the need for antifouling coatings has become the highlight of research during recent years. Nowadays, the most commonly used antifouling agent includes Irgarol, Diuron, copper pyrrithione, zinc pyrrithione, and 4,5-dichloro-2-*n*-octyl-4-isothiazolin-3-one (DCOIT) as the successors for tributyltin (TBT) compound, which was banned due to its toxicity.^{2,3} However, recent studies have shown the toxicity of these antifouling agents: Irgarol,^{4,5} Diuron,⁶ DCOIT,^{7,8} and copper and zinc pyrrithiones^{9,10} that can potentially cause severe negative environmental impact. To eliminate the use of toxic biocides, alternative environmentally friendly solutions such as bioinspired surface^{11,12} and surface chemistry^{13,14} were introduced. Additionally, the use of natural antimicrobial compound has become one of the options that can potentially solve this problem.

Essential oils (EOs) produced from plant extracts have gained wide attention recently due to their multifunctional properties such as antimicrobial, antioxidant, antifungal, anti-inflammatory, and mosquito repellent.¹⁵ Among all these

properties, the antimicrobial function of EOs was studied intensively, because bacteria can be found everywhere and frequently cause severe problems, especially to human health.^{16,17} Clove oil is an essential oil extracted from *Syzygium aromaticum* that exhibits significant antimicrobial effects against a wide range of bacterial strains.¹⁸ In addition to antimicrobial effect, clove oil possesses antibiofilm,^{19,20} antioxidant,²¹ antifungal,²² anti-inflammatory,²³ antiviral,²⁴ and insect repellent activity.²⁵ However, clove oil has several disadvantages, including its volatility^{26,27} and chemical instability²⁸ under the presence of light, air, and high temperature, which have severely limited its practical applications. Hence, encapsulation serves as a means to protect clove oil from the harsh surrounding environment and prevent premature release and degradation of clove oil.

Recently, several techniques were applied to encapsulate clove oil. Encapsulation of clove oil was accomplished by using liposomes,²⁹ single coagulation,³⁰ spray dried,³¹ coacervation phase,³² and envelope binding methods.³³ However, on the basis of the characterization of the synthesized microcapsules, high agglomeration tendency and irregular shape of the

Received: April 5, 2018

Accepted: April 23, 2018

Published: April 23, 2018

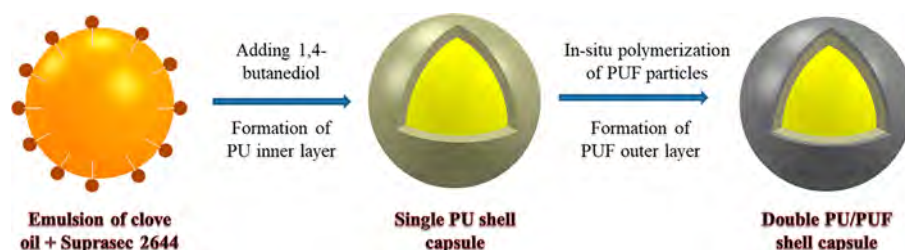


Figure 1. Schematic fabrication process of double PU/PUF layer microcapsules containing clove oil.

microcapsules remain a challenge for the aforementioned microencapsulation techniques. Irregular shapes and agglomeration problems affect undesirably the delivery and release of the encapsulated core. In contrast, polymer microencapsulation techniques were proven to produce robust microcapsules with regular shapes, which are used extensively in a wide range of applications.^{34–41} In this study, interfacial and in situ polymerization techniques are utilized to fabricate microcapsules containing clove oil.

Previous studies have shown great uses of clove oil in different applications, mainly in the food industry as antimicrobial and antioxidant compound. However, there has not been any study on the effect of clove oil against marine bacteria. Furthermore, insufficient release of clove oil can cause ineffectiveness, while excessive release results in skin irritation and negative impacts to human health. Hence, the understanding of the release behavior of clove oil from microcapsules is essential. By manipulating the shell thickness and surface morphology, a double-layer shell structure allows the control over both shells to achieve different release profiles required for different applications. To our knowledge, this study is the first to fabricate double-layer shell antibacterial microcapsules containing essential oils and systematically investigate the release profile of the microcapsules by tuning the shell thickness and surface morphology of the shells. This study will provide insight into tuning the release profile of double-layer shell microcapsules by manipulating parameters related to the shell thickness and surface morphology of the microcapsules. Antibacterial test of these microcapsules against different kinds of bacteria including marine bacteria shows their potential as the environmentally friendly solution to replace existing toxic antifouling agent.

MATERIALS AND METHODS

Materials. 4,4-Diphenylmethane diisocyanate (MDI) prepolymer Suprasec 2644 was obtained from Huntsman. Gum Arabic, formaldehyde solution (35–37 wt %), urea, resorcinol, ammonium chloride, 1,4-butanediol (BDO), clove oil, sodium hydroxide (NaOH), and hydrochloric acid (HCl, 0.1 M) were purchased from Sigma-Aldrich. The sterile surface swab kit was purchased from SKC Asia. Marine broth 2216 and marine agar 2216 were purchased from BD, Difco.

Synthesis of Microcapsules. Microcapsules containing clove oil were fabricated through a combination of interfacial and in situ polymerization. The whole process is illustrated in Figure 1. In the first step, interfacial polymerization was employed to fabricate the inner polyurethane (PU) shell of the microcapsules. A solution of 50 mL of deionized (DI) water with 3 wt % of gum Arabic as surfactant was prepared and heated to 40 °C in a 250 mL beaker that was immersed in a temperature-controlled water bath. Under an agitation rate of 800 rpm, the oil-phase mixture of 2 g of Suprasec 2644 and 10 g of clove oil was added dropwise into the above surfactant solution, and the ensuing emulsification was allowed to take place for 20 min. Next, 2 g

of BDO was then added slowly into the system to initiate interfacial polymerization to form the PU inner shell.

Subsequently, in situ polymerization was applied to form the outer poly(urea-formaldehyde) (PUF) shell of the microcapsules. Two grams of urea, 0.5 g of ammonium chloride, and 0.5 g of resorcinol were dissolved in 60 mL of DI water and heated to 55 °C in a 250 mL beaker immersed in water bath. This was followed by adjusting the pH value of the system to 3.5 through addition of NaOH and HCl solutions. Next, the polyurethane microcapsules from the first step were dispersed into the system followed by adding 5 g of 37 wt % formaldehyde solution to initiate the in situ polymerization reaction. The system was left to react for 30 min before rinsing with DI water several times and air drying for 12 h before future characterization.

Characterization of Microcapsules. The morphologies, size, core-shell structure, and shell thickness of obtained microcapsules were observed through field emission scanning electron microscope (FESEM; Joel, model JSM-7600F). First, the microcapsules were scattered on conductive tape. Some of them were then lightly crushed with a razor blade, so that the cross-section and inner structure of the shell can be observed. Meanwhile, the size distributions of the microcapsules were calculated using ImageJ based on at least 150 specimens.

Determination of Microcapsules Content. Fourier Transform infrared (FTIR) spectra were obtained using FTIR spectrometer to examine the chemical structure of the microcapsules. The testing samples were prepared by grinding the microcapsules with potassium bromide (KBr), followed by transmitting infrared light through the samples to scan and observe the chemical properties of the microcapsules. Different samples, including pure clove oil, microcapsules containing clove oil and PU/PUF shell material, were examined using FTIR spectroscopy to confirm successful encapsulation of clove oil.

Core Fraction. The core content of the prepared microcapsules was determined by the extraction method using ethanol as the extracting solvent. Initially, 0.1 g of microcapsules (W_1) was weighed and poured into a folded filter paper. The microcapsules were subsequently squeezed firmly to completely release the encapsulated clove oil. Then, the clove oil was extracted from the broken microcapsules using ethanol. The extraction process was repeated five times to ensure complete extraction, and the remaining weight (W_2) of shell material was measured carefully. This extraction test was conducted three to five times to determine the average value. Lastly, the calculation of core content is based on the equation below:

$$\text{core content (\%)} = \frac{W_1 - W_2}{W_1} \times 100 \quad (1)$$

Controlled Release Study. The release of clove oil from the microcapsules was characterized using ultraviolet–visible (UV–vis) spectroscopy. Initially, microcapsules containing clove oil were placed in a dialysis bag that was subsequently submerged in a centrifuge tube with DI water as the dissolution medium. At different time intervals, 2 mL aliquots were taken out, and an equal amount of fresh DI water was added into the centrifuge tube. Subsequently, the solution samples at different time intervals were analyzed for their clove oil content using UV–vis spectrophotometer (at $\lambda = 280$ nm), and the amount of clove oil released was calculated based on Beer–Lambert law. To

ensure consistency and accuracy of results, all measurements were performed in triplicate.

Preparation of Marine Biofilm-Forming Bacteria. To examine the antibacterial activities against the marine biofilm forming bacteria, marine biofilm was prepared by immersing a steel plate with epoxy coating (5 cm × 5 cm × 1 cm) in natural seawater near Sebarok island in Singapore. After immersion in the natural seawater for two weeks, the steel plate was collected and washed aseptically with filtered seawater several times to remove the unattached bacteria. Subsequently, a sterile surface swab was rubbed across the sampling area of 5 cm × 5 cm to scrape the marine biofilm-forming bacteria from the sample surface. These bacteria on the surface swab were then suspended in the marine broth 2216 and grown overnight at 30 °C. The composition of marine broth and marine agar 2216 is shown in Table 1.

Table 1. Composition of Marine Agar 2216 and Marine Broth 2216 (without Agar)

composition	formulation (g/L)	composition	formulation (g/L)
sodium chloride	19.45	potassium bromide	0.08
magnesium chloride	8.8	strontium chloride	0.034
peptone	5.0	boric acid	0.022
sodium sulfate	3.24	disodium phosphate	0.008
calcium chloride	1.8	sodium silicate	0.004
yeast extract	1.0	sodium fluoride	0.0024
potassium chloride	0.55	ammonium nitrate	0.0016
sodium bicarbonate	0.16	agar	15
ferric citrate	0.1		

Antibacterial Test. The antibacterial activities of the fabricated microcapsules containing clove oil were evaluated based on ASTM E2315 against *Vibrio coralliilyticus*, *Exiguobacterium aestuarii*, *Escherichia coli*, and the collected marine biofilm-forming bacteria using a time-kill test method.⁴² Cultures of *V. coralliilyticus*, *E. aestuarii*, and *E. coli* were prepared overnight at 30 °C in marine broth 2216. The bacterial suspensions were all diluted in phosphate-buffered saline (PBS) solution to a concentration of $\sim 1 \times 10^6$ cfu/ml as the starting bacteria concentration for the time-kill test. Meanwhile, 0.2 g of microcapsules containing clove oil was placed in a dialysis bag with 2 mL of DI water. Subsequently, this dialysis bag containing microcapsules was brought into contact with 20 mL of prepared PBS solution containing 1×10^6 cfu/ml of *V. Coralliilyticus*, *E. aestuarii*, and *E. coli*, respectively, at room temperature. For the marine biofilm-forming bacteria, 0.4 g of microcapsules containing clove oil was used to treat a wider range of marine bacteria in the suspension, which may require different minimum inhibition concentration (MIC) values. At different time intervals, an aliquot was removed, and appropriate dilutions were made using PBS solution. The standard plate count method was adopted, whereby the diluted bacterial suspension was spread uniformly on marine agar 2216 plates. The plates were incubated overnight at 30 °C before quantification of the number of colony forming unit (CFU) to determine the surviving organisms. According to the results, the antibacterial activities of microcapsules containing clove oil can be determined and compared between different formulations.

RESULTS AND DISCUSSION

Morphology of Microcapsules and Shell Structure. It can be seen from Figure 2 that the resultant microcapsules are spherical in shape with an average diameter of $102.2 \pm 17.3 \mu\text{m}$ (measured using software ImageJ). The size distribution of the microcapsules based on 150 individual microcapsules is shown in Figure 2d. Figure 2c shows the cross-sectional view of the

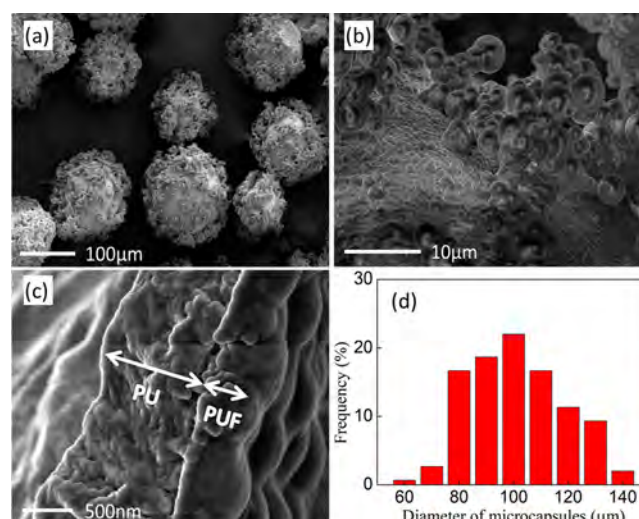


Figure 2. (a) Overview of double PU/PUF shell microcapsules containing clove oil; (b) shell morphology of individual microcapsule; (c) cross-sectional view of the shell showing inner porous PU and outer dense PUF shells; (d) histogram of the microcapsule diameter distribution.

broken shell, consisting of an inner porous PU layer and an outer dense PUF layer. This confirms the existence of a core-shell structure of the microcapsules with distinctive layers of PU and PUF in the shell. It is apparent that the outer surface of the microcapsules is very rough due to the dense deposition of urea-formaldehyde (UF) nanoparticles, while the inner PU layer of the microcapsules appears to be more porous and loose as shown in Figure 3a1–a3. The overall shell thickness of the double-layer PU/PUF microcapsules is $\sim 1.2 \mu\text{m}$, which consists of a $0.86 \pm 0.16 \mu\text{m}$ inner PU layer and a $0.41 \pm 0.07 \mu\text{m}$ outer PUF layer. Figure 2c shows the cross-sectional view of the shell, consisting of an inner porous PU layer and an outer dense PUF layer.

Formation Mechanisms of Double-Layered Shell. The mixture of clove oil and PU prepolymer in the oil phase was emulsified into finer liquid droplets in a 3 wt % gum Arabic surfactant aqueous solution. Gum Arabic contains glycoprotein and polysaccharides. The content of glycoprotein contains amino functional group and tends to react with isocyanates.⁴³ After 20 min of emulsification, a thin shell was formed at the oil/water interface. However, the structure of this thin shell is very loose, and it collapses in less than half an hour under exposure to the environment. Some BDO was then added into the continuous phase to react with PU prepolymer at the oil-water interface to form a PU shell through the reaction between NCO groups in the PU prepolymer and OH groups in the diol.⁴⁴ A reaction time of 3 h was utilized to allow diffusion of diol across the PU shell for further shell thickening. However, the single-layer PU shell is porous, and the release of clove oil from this porous PU shell is rapid. Additionally, the microcapsules tend to aggregate upon drying due to the leakage of clove oil from the porous PU shell. According to Figure 3a1, the inner PU layer is formed through agglomeration of PU nanoparticles, which are the result of the reaction between isocyanates and diol. Hence, the voids between these nanoparticles contribute to a porous PU layer, which eventually allows rapid release of clove oil across the shell membrane. Moreover, the single-layer PU shell has low mechanical strength due to its loose and porous structure. On the basis

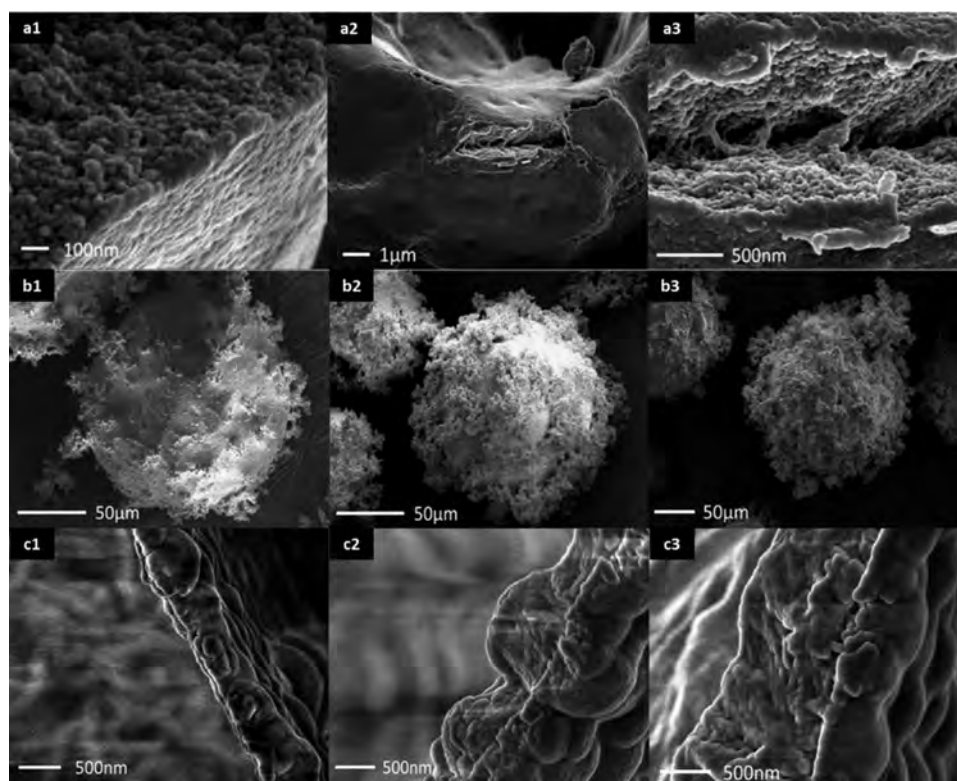


Figure 3. FESEM images indicating low mechanical strength of PU shell: (a1) inner PU layer consists of PU nanoparticles across the shell; (a2) crack observed on single-layer PU shell; (a3) magnification of the crack indicating low mechanical strength. FESEM images of microcapsules fabricated under different parameters: (b1–b3) increasing roughness of surface morphology at increasing length of PUF deposition time; (c1–c3) increasing PU shell thickness at increasing amount of PU reactants.

of Figure 3a2, some cracks were observed on the microcapsules after storage in the vial for several days. Hence, a second layer of cross-linked polymer was fabricated to decrease and control the release rate and prolong the service lifetime of these microcapsules.

Under an acidic condition, urea-formaldehyde tends to polymerize at 55 °C. This behavior was used in a polymerization technique to fabricate microcapsules with a dense PUF shell.⁴⁵ At pH 3.5 and a reaction temperature of 55 °C, the polymerization process was initiated as soon as formaldehyde solution was added into the solution containing urea. As the molecular weight of PUF increases, it starts to deposit on the PU shell. With increasing reaction time for UF deposition, microcapsules with higher surface roughness can be formed. The rougher surface of these microcapsules can contribute to super-hydrophobic properties for the use of different applications including self-cleaning and antifouling coatings.²³

Influence of Reaction Parameters. *A.I. Length of PUF Reaction Time.* In this study, the influence of the length of PUF reaction time on the surface morphology of the final microcapsules was investigated. As shown in Figure 3b1–b3, the surface morphology of the microcapsules becomes rougher as the PUF deposition time increases. It is apparent that the amount of PUF nanoparticles deposited on the initial PU shell has increased significantly when the PUF reaction time is prolonged from 15 min to 1 h. This phenomenon is related to the formation mechanism of PUF shell, which depends on the deposition of PUF nanoparticles through in situ polymerization under acidic environment. As the reaction time is prolonged, PUF nanoparticles with increasing molecular weight start to deposit on the PU shell to form a dense shell with rough

surface morphology. Tuning the surface morphology by controlling the length of PUF reaction time is important to manipulate the release profile of the microcapsules, which will be discussed later in this study.

A.II. Amount of PU Reactants. The influence of the amount of PU reactants on the inner PU shell thickness of the microcapsules was studied. Figure 3c1–c3 shows the increase of PU shell thickness with increasing amount of PU reactants added. The amount of PU reactants (Suprasec 2644 and BDO) added was 1, 2, and 3 g each, respectively, resulting in PU shell thickness of 252 ± 82 , 444 ± 122 , and 859 ± 161 nm as shown in Figure 4. This phenomenon is relevant to the formation mechanism of PU shell through interfacial polymerization.

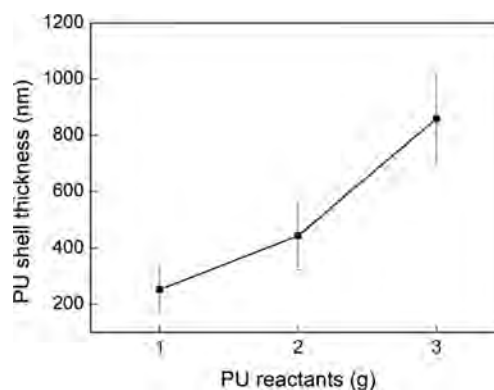


Figure 4. Effect of the amount of PU reactants (Suprasec 2644 and BDO) added on the PU shell thickness of the fabricated microcapsules.

During the interfacial polymerization process, clove oil as the core material was mixed well with MDI-based urethane prepolymer Suprasec 2644 to form the oil phase. Addition of chain extender BDO in the aqueous phase initiated the polymerization reaction at the oil–water interface, through the reaction between the hydroxyl group in the aqueous phase and the isocyanate group in the oil phase. Hence, the thickness of the PU layer increases when higher amount of diol in the aqueous phase diffuses across the initial membrane to react with higher amount of isocyanates. The control over the PU shell thickness through changing the amount of PU reactants is important to tune the release profile of the microcapsules, which will be discussed later.

Determination of Microcapsules Content. FTIR spectra of pure clove oil, core material extracted from the microcapsules, and shell material are shown in Figure 5. It can be

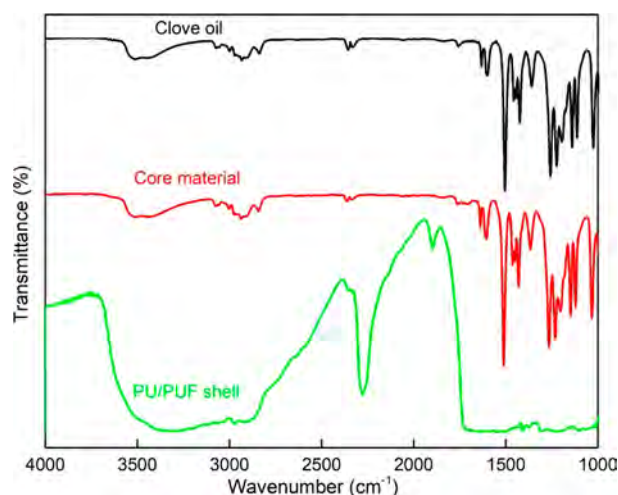


Figure 5. FTIR spectra of clove oil, double-layered PU/PUF shell, and core material (clove oil). Identical spectra of clove oil and core material confirm successful encapsulation of clove oil.

seen that the spectrum of clove oil is similar to that of core material extracted from the microcapsules containing clove oil using acetone, indicating that clove oil was successfully encapsulated. The absorption band in the region from 3000 to 3500 cm^{-1} represents the OH stretching in clove oil. For the spectrum of PU/PUF shell, the absorption band at 2260 cm^{-1} represents the NCO stretch characteristics. This indicates that the NCO functional groups in the shell were not exhausted completely during the reaction process and that the highly

cross-linked PUF outer layer prevents its diffusion across the shell to react with water molecules outside.⁴⁶

Core Fraction of Microcapsules. The solvent extraction method was used to measure the core fractions of the microcapsules fabricated under different parameters. Figure 6 shows the core fractions of microcapsules fabricated using different amounts of PU reactants and different lengths of PUF deposition time. On the basis of Figure 6a, higher amount of PU reactants decreases the core fraction of the microcapsules. Higher amount of PU reactants contributes to thicker PU shell, which increases the overall weight of the microcapsules. As a result, the fraction of clove oil encapsulated is comparatively lower. Longer PUF deposition time also decreases the core fraction of the microcapsules as shown in Figure 6b. With longer PUF deposition time, the deposition of PUF nanoparticles increases and creates a relatively rougher surface structure. Similar to the PU reactants scenario, these PUF nanoparticles increase the overall weight of the microcapsules and decrease the fraction of clove oil encapsulated. By manipulating these two parameters, the release behavior of clove oil from the microcapsules can be tuned, and this will be discussed in the following section.

Controlled Release Study. Environmental impact of chemicals used for various applications has become an important issue to be addressed. Insufficient release may compromise the performance of targeted applications, while rapid release can shorten the lifetime of the microcapsules. Hence, knowledge about the release rate of clove oil from the microcapsules is essential before the implementation stage. Additionally, the ability to control the release rate creates flexibility to design appropriate release behavior for the needs of different applications. In this study, the amount of PU reactants and reaction time for PUF shell formation were studied to investigate their influences on the release rate. FESEM images of microcapsules fabricated under different parameters are shown to further explain the release behavior.

Over the past few decades, significant advances have been achieved in the field of drug release, and several different models were derived to explain different release behavior of different dosage forms. In this study, several release models were compared, which include zero-order,⁴⁷ Ritger–Peppas,^{48,49} Higuchi,^{50,51} and Baker–Lonsdale⁵² models.

Zero-order model:

$$\frac{M_t}{M_\infty} = kt \quad (2)$$

where k is the zero-order constant.

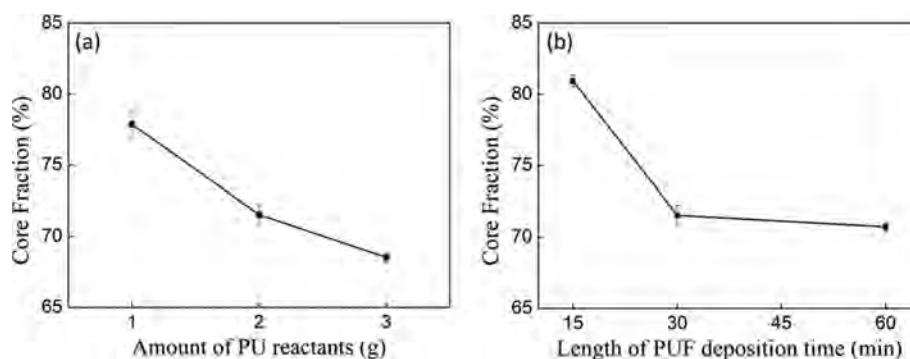


Figure 6. Core content of microcapsules fabricated under different parameters: (a) amount of PU reactants and (b) length of PUF deposition time.

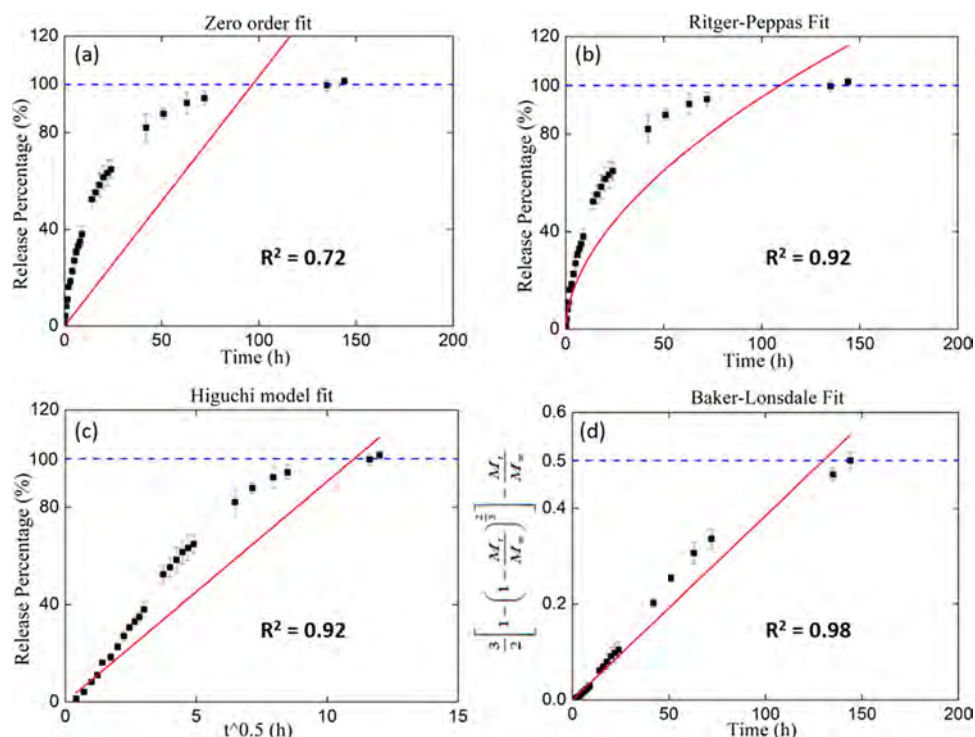


Figure 7. Fitting of release profile using different models: (a) Zero-order model, (b) Ritger–Peppas model, (c) Higuchi model, (d) Baker–Lonsdale model and the correlation coefficients of corresponding kinetic models.

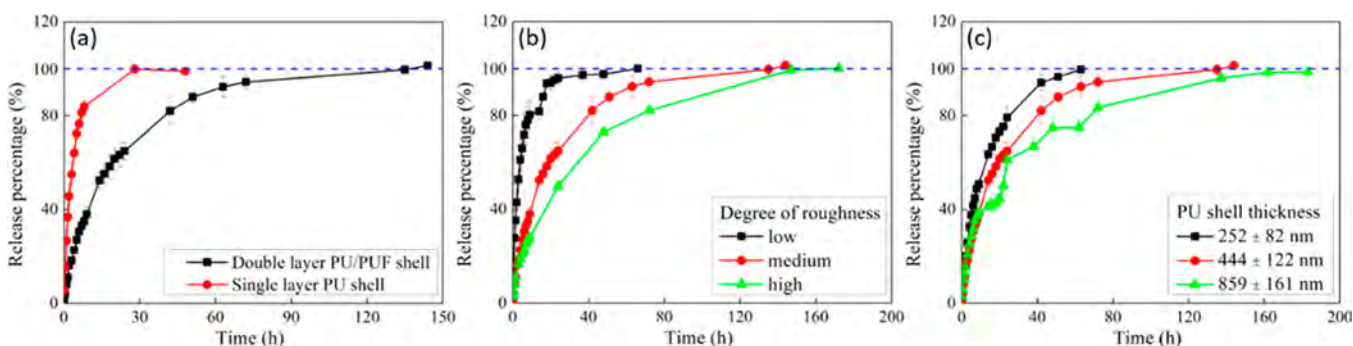


Figure 8. Influence of (a) the number of shell layers; (b) the morphology of PUF shell; (c) the PU shell thickness on release profiles.

Ritger–Peppas model:

$$\frac{M_t}{M_\infty} = at^n \quad (3)$$

where a is a constant, and n is the release exponent.

Higuchi model:

$$\frac{M_t}{M_\infty} = k_H t^{0.5} \quad (4)$$

where k_H is the Higuchi dissolution constant.

Baker–Lonsdale Model:

$$\frac{3}{2} \left[1 - \left(1 - \frac{M_t}{M_\infty} \right)^{2/3} \right] - \frac{M_t}{M_\infty} = \frac{3D_m C_{ms}}{r_0^2 C_0} t = k_B t \quad (5)$$

where D_m is the diffusion coefficient, C_{ms} is the drug solubility in the matrix, r_0 is the radius of the microcapsules, M_t is the released amount at time t , M_∞ is the total amount released, and C_0 is the initial drug concentration in the matrix. In this study,

k_B is the Baker–Lonsdale constant, which is used to fit the release profile.

According to Figure 7, the release profile of the double-layer PU/PUF microcapsules is fitted best to the Baker–Lonsdale model with the highest R -squared value. This model was derived from the Higuchi model to describe the drug release behavior specifically for microcapsules and microspheres.⁵² On the basis of this model, the release mechanism from these double-layer PU/PUF shell microcapsules is determined to be primarily diffusion across the polymeric shell.

Influence of Shell Structure on the Release Profile.

B.I. Single and Double-Layer Shell. The release profiles of microcapsules with double-layer PU/PUF shell and single-layer PU shell are shown in Figure 8a, with slower release rate of clove oil from double-layer PU/PUF shell microcapsules. Owing to the dense structure of PUF layer, the release of clove oil from the microcapsules is prolonged, and complete release takes approximately one week, much longer as compared to single PU layer microcapsules, which take only 1 d to completely release the encapsulated clove oil.

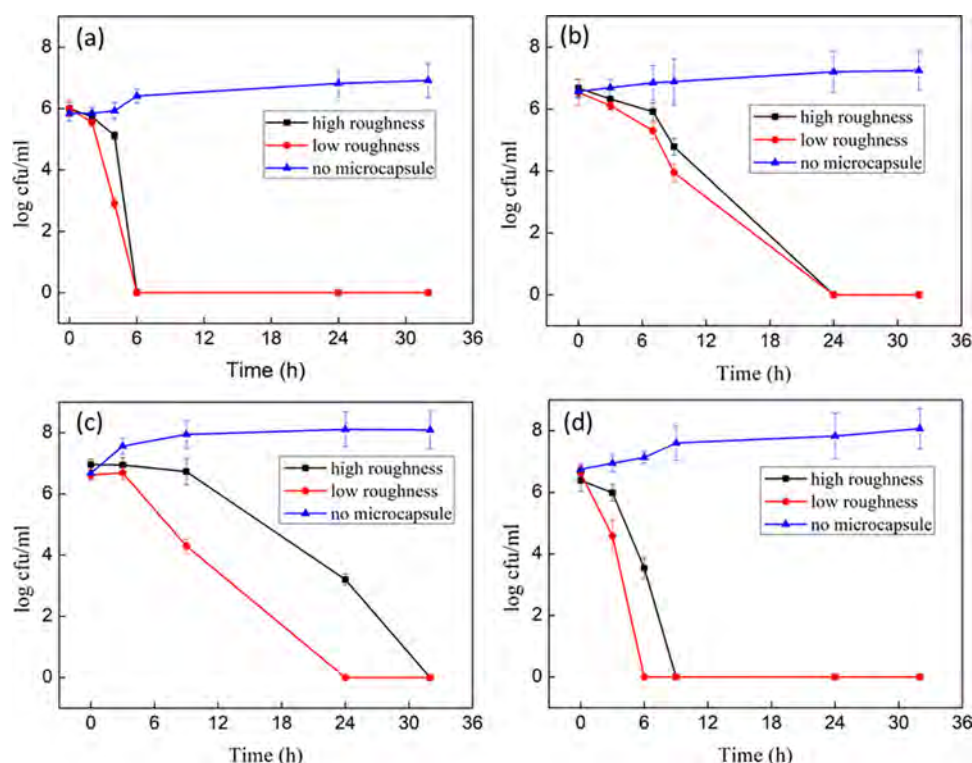


Figure 9. Antibacterial time-kill test results of fabricated microcapsules containing clove oil with different surface roughness against (a) *V. coralliilyticus*, (b) *E. aestuarii*, (c) *E. coli*, and (d) marine biofilm-forming bacteria isolated from on-site contaminated samples.

As shown in Figure 3a1–a3, the porous structure and poor mechanical strength of the single-layer PU shell leads to some cracks, which decrease the shelf life of these microcapsules. Additionally, the porous structure of the PU shell results in premature release of clove oil, which can eventually cause severe microcapsule agglomeration and halt further process for potential industrial application. To prolong the release of clove oil and extend the lifetime of these microcapsules, another layer of dense PUF shell was deposited through in situ polymerization. As shown in Figure 2c, distinctive layers of PU and PUF shells were observed. It is apparent that the additional PUF shell increases the overall shell thickness of the microcapsules and prevents premature release of the clove oil.

B.II. Morphology of PUF Layer in Double Shell. The release profiles in Figure 8b demonstrate the effect of PUF reaction time on the release rate of clove oil from the microcapsules. In particular, the release profile of the microcapsules with 15 min of PUF reaction time shows the highest release rate, and complete release occurs in less than 2 d. By increasing the PUF reaction time to 30 min and 1 h, the release rate is significantly lower, and the complete release only occurs after a week of immersion in water.

The difference in the release rate of these microcapsules is related to the microcapsule surface morphology. As shown in Figure 3b1–b3, the surface morphology of the microcapsules can be modified through manipulating the PUF reaction time. As the PUF reaction time increases, the in situ polymerization of PUF nanoparticles extends, and more PUF nanoparticles are allowed to deposit on the shell. The PUF nanoparticles' stacking contributes to a rougher surface and increases the diffusion distance of clove oil across the shell membrane. As the diffusion of clove oil occurs from every dimension of the spherical microcapsules, rougher surface morphology sustains

the release of clove oil and decreases the release rate of clove oil at longer PUF reaction time.

B.III. Thickness of PU Layer in Double Shell. As shown in Figure 3c1–c3, the PU shell thickness can be controlled by varying the amount of PU reactants. It is evident from the FESEM images that the thickness of the PU shell can be increased through increasing the amount of PU reactants. Additionally, this change in PU shell thickness can be utilized to control the release profiles of the microcapsules. According to the release profiles shown in Figure 8c, the release rate of clove oil is slowed by increasing the amount of PU reactants added.

The thickness of PU shell is essential in controlling the release rate of clove oil, as thicker shell increases the distance clove oil requires to diffuse before being released from the microcapsules, rendering them with slower release rate. The release profiles and FESEM images of the microcapsules fabricated through adding different amounts of PU reactants have successfully proven the feasibility of controlling PU shell thickness and fabricating microcapsules with different release rate.

Antibacterial Activity. Bacteria species belonging to genera *Vibrio* were usually used as the representative of marine bacteria to test the effectiveness of antifouling agents or paint coatings.⁵³ *V. coralliilyticus* is a globally distributed bacterium with temperature-dependent pathogenicity in coral and was found in marine biofilm.⁵⁴ Hence, antibacterial activity of fabricated microcapsules against *V. coralliilyticus* is a preliminary indication on the potential to treat biofouling. Additionally, *Exiguobacterium* is another species isolated from the marine biofilm,^{55,56} and hence, *E. aestuarii* isolated from the marine environment is used in this study as another representative of marine bacteria. Furthermore, *E. coli* was found in the marine biofilm on the ship hulls.⁵⁷ As a result, these three bacteria are

used as the individual bacteria associated with the formation of marine biofilm. Additionally, the marine biofilm-forming bacteria collected from the on-site contaminated sample serves as a comprehensive indication of the effectiveness of the fabricated microcapsules in treating biofouling problem.

Figure 9 summarizes the antibacterial time-kill test results of the fabricated microcapsules with different surface roughness against *V. coralliilyticus*, *E. aestuarii*, *E. coli*, and marine biofilm-forming bacteria isolated from on-site contaminated sample. As discussed previously, a shorter length of PUF deposition time results in a low roughness outer surface morphology of the microcapsules. Because of the faster release rate of clove oil from the microcapsules with low roughness, the antibacterial activity was observed earlier as shown in Figure 9. According to the antibacterial test results of all the marine bacteria tested, the antibacterial activity of the fabricated microcapsules was proven to be affected by the release rate of clove oil from the fabricated microcapsules with different surface roughness. Specifically, the complete killing of the bacteria for microcapsules with low roughness occurs at a much earlier contact time as compared to that for microcapsules with high roughness. Meanwhile, the bacteria remain viable for the control sample without the addition of the fabricated microcapsules, indicating the entire antibacterial mechanism as a result of the released clove oil from the fabricated microcapsules.

On the basis of the time-kill tests against the individual marine bacteria and the marine biofilm-forming bacteria isolated from the on-site contaminated samples, it was shown that the release rate of clove oil affects greatly the antibacterial activity of the fabricated microcapsules. On the basis of previous research, the antibacterial activity of eugenol as the main component in clove oil was proven through its ability to disrupt and permeabilize the cell membrane.^{58–60} The increasing transport of potassium and adenosine triphosphate (ATP) out of the cells causes cell death eventually.⁶¹ Hence, in this antibacterial study, the release rate of clove oil influences the frequency of interaction between eugenol and the cell membrane, thus affecting the duration required to completely kill the bacteria. In summary, microcapsules with different surface roughness exhibit antibacterial function with different release profile, proving its versatility for different applications requiring different release and bacteria killing rates.

CONCLUSION

In summary, double-layered PU/PUF shell microcapsules containing clove oil have been successfully fabricated through interfacial and in situ polymerization methods. The release profile can be tuned through the change in PU shell thickness and the microcapsules surface morphology by manipulating the amount of PU reactants added and the length of PUF deposition time, respectively. Additionally, the potential use of the fabricated microcapsules containing clove oil for antifouling applications was examined through the antibacterial test against different individual marine bacteria, which include *V. coralliilyticus*, *E. aestuarii*, and *E. coli*. According to the time-kill test, the microcapsules show excellent antibacterial activity against all the bacterial strains with different killing rate for microcapsules with different surface roughness, indicating the versatility of these microcapsules for different applications that may require different release and bacteria killing rates. Remarkably, the antibacterial activity of these microcapsules against the marine biofilm-forming bacteria isolated from the on-site contaminated samples proves their great potential to

serve as a new environmentally friendly solution to replace the existing toxic antifouling agent.

AUTHOR INFORMATION

Corresponding Authors

*E-mail: maeyang@ust.hk. Phone: +852 3469 2298. (J.-L.Y.)

*E-mail: mcyue@ntu.edu.sg. Phone: +65 6592 2696. (C.Y.Y.)

ORCID

Yong-Bing Chong: 0000-0003-1681-0246

Chee Yoon Yue: 0000-0003-3729-1668

Jinglei Yang: 0000-0002-9413-9016

Notes

The authors declare no competing financial interest.

ACKNOWLEDGMENTS

We are grateful for the support partially from the Hong Kong Univ. of Science and Technology (Grant No. R9365). Y.-B.C. acknowledges the research scholarship support from NTU and is grateful for the assistance and discussion with Prof. Shearwood at MAE@NTU. Y.-B.C. also would like to acknowledge Dr. K. P. Ramasamy from SCELSE@NTU for providing the marine bacteria isolates. Y.-B.C. appreciates the kind help from Mr. Nicholas Lee and Singapore Cleanseas Pte Ltd for their support on the on-site contaminated sample collection.

REFERENCES

- (1) Lindholdt, A.; Dam-Johansen, K.; Olsen, S.; Yebra, D. M.; Kiil, S. Effects of biofouling development on drag forces of hull coatings for ocean-going ships: a review. *Journal of Coatings Technology and Research* **2015**, *12* (3), 415–444.
- (2) Huggett, R. J.; Unger, M. A.; Seligman, P. F.; Valkirs, A. O. ES&T Series: The marine biocide tributyltin. Assessing and managing the environmental risks. *Environ. Sci. Technol.* **1992**, *26* (2), 232–237.
- (3) Landmeyer, J. E.; Tanner, T. L.; Watt, B. E. Biotransformation of tributyltin to tin in freshwater river-bed sediments contaminated by an organotin release. *Environ. Sci. Technol.* **2004**, *38* (15), 4106–4112.
- (4) Thomas, K. V.; McHugh, M.; Waldo, M. Antifouling paint booster biocides in UK coastal waters: inputs, occurrence and environmental fate. *Sci. Total Environ.* **2002**, *293* (1–3), 117–127.
- (5) Mohr, S.; Berghahn, R. d.; Mailahn, W.; Schmiediche, R.; Feibicke, M.; Schmidt, R. Toxic and accumulative potential of the antifouling biocide and TBT successor Irgarol on freshwater macrophytes: a pond mesocosm study. *Environ. Sci. Technol.* **2009**, *43* (17), 6838–6843.
- (6) Giacomazzi, S.; Cochet, N. Environmental impact of diuron transformation: a review. *Chemosphere* **2004**, *56* (11), 1021–1032.
- (7) Bellas, J. Comparative toxicity of alternative antifouling biocides on embryos and larvae of marine invertebrates. *Sci. Total Environ.* **2006**, *367* (2–3), 573–585.
- (8) Chen, L.; Au, D. W.; Hu, C.; Peterson, D. R.; Zhou, B.; Qian, P.-Y. Identification of Molecular Targets for 4, 5-Dichloro-2-n-octyl-4-isothiazolin-3-one (DCOIT) in Teleosts: New Insight into Mechanism of Toxicity. *Environ. Sci. Technol.* **2017**, *51* (3), 1840–1847.
- (9) Okamura, H.; Watanabe, T.; Aoyama, I.; Hasobe, M. Toxicity evaluation of new antifouling compounds using suspension-cultured fish cells. *Chemosphere* **2002**, *46* (7), 945–951.
- (10) Almond, K. M.; Trombetta, L. D. The effects of copper pyrrithione, an antifouling agent, on developing zebrafish embryos. *Ecotoxicology* **2016**, *25* (2), 389–398.
- (11) Huang, C.-J.; Chu, S.-H.; Wang, L.-C.; Li, C.-H.; Lee, T. R. Bioinspired Zwitterionic Surface Coatings with Robust Photostability and Fouling Resistance. *ACS Appl. Mater. Interfaces* **2015**, *7* (42), 23776–23786.

- (12) Cho, J. H.; Shanmuganathan, K.; Ellison, C. J. Bioinspired Catecholic Copolymers for Antifouling Surface Coatings. *ACS Appl. Mater. Interfaces* **2013**, *5* (9), 3794–3802.
- (13) Knowles, B. R.; Wagner, P.; MacLaughlin, S.; Higgins, M. J.; Molino, P. J. Silica Nanoparticles Functionalized with Zwitterionic Sulfobetaine Siloxane for Application as a Versatile Antifouling Coating System. *ACS Appl. Mater. Interfaces* **2017**, *9* (22), 18584–18594.
- (14) Zhu, X.; Jańczewski, D.; Guo, S.; Lee, S. S. C.; Parra Velandia, F. J.; Teo, S. L.-M.; He, T.; Puniredd, S. R.; Vancso, G. J. Polyion Multilayers with Precise Surface Charge Control for Antifouling. *ACS Appl. Mater. Interfaces* **2015**, *7* (1), 852–861.
- (15) Sacchetti, G.; Maietti, S.; Muzzoli, M.; Scaglianti, M.; Manfredini, S.; Radice, M.; Bruni, R. Comparative evaluation of 11 essential oils of different origin as functional antioxidants, antiradicals and antimicrobials in foods. *Food Chem.* **2005**, *91* (4), 621–632.
- (16) Calo, J. R.; Crandall, P. G.; O'Bryan, C. A.; Ricke, S. C. Essential oils as antimicrobials in food systems—A review. *Food Control* **2015**, *54*, 111–119.
- (17) Burt, S. Essential oils: their antibacterial properties and potential applications in foods—a review. *Int. J. Food Microbiol.* **2004**, *94* (3), 223–53.
- (18) Dorman, H. J. D.; Deans, S. G. Antimicrobial agents from plants: antibacterial activity of plant volatile oils. *J. Appl. Microbiol.* **2000**, *88* (2), 308–316.
- (19) Cui, H.; Ma, C.; Lin, L. Synergetic antibacterial efficacy of cold nitrogen plasma and clove oil against *Escherichia coli* O157:H7 biofilms on lettuce. *Food Control* **2016**, *66*, 8–16.
- (20) Cui, H.; Bai, M.; Rashed, M. M. A.; Lin, L. The antibacterial activity of clove oil/chitosan nanoparticles embedded gelatin nanofibers against *Escherichia coli* O157:H7 biofilms on cucumber. *Int. J. Food Microbiol.* **2018**, *266*, 69–78.
- (21) Shan, B.; Cai, Y. Z.; Sun, M.; Corke, H. Antioxidant capacity of 26 spice extracts and characterization of their phenolic constituents. *J. Agric. Food Chem.* **2005**, *53* (20), 7749–7759.
- (22) Kalemba, D.; Kunicka, A. Antibacterial and antifungal properties of essential oils. *Curr. Med. Chem.* **2003**, *10* (10), 813–829.
- (23) Darshan, S.; Doreswamy, R. Patented antiinflammatory plant drug development from traditional medicine. *Phytother. Res.* **2004**, *18* (5), 343–357.
- (24) Hussein, G.; Miyashiro, H.; Nakamura, N.; Hattori, M.; Kakiuchi, N.; Shimotohno, K. Inhibitory effects of Sudanese medicinal plant extracts on hepatitis C virus (HCV) protease. *Phytother. Res.* **2000**, *14* (7), 510–516.
- (25) Trongtokit, Y.; Curtis, C. F.; Rongsriyam, Y. Efficacy of repellent products against caged and free flying *Anopheles stephensi* mosquitoes. *Southeast Asian J. Trop. Med. Public Health* **2005**, *36*, 1423–1431.
- (26) Edris, A. E. Pharmaceutical and therapeutic Potentials of essential oils and their individual volatile constituents: a review. *Phytother. Res.* **2007**, *21* (4), 308–323.
- (27) Bullerman, L. B.; Lieu, F. Y.; Seier, S. A. INHIBITION OF GROWTH AND AFLATOXIN PRODUCTION BY CINNAMON AND CLOVE OILS. CINNAMIC ALDEHYDE AND EUGENOL. *J. Food Sci.* **1977**, *42* (4), 1107–1109.
- (28) Turek, C.; Stintzing, F. C. Stability of essential oils: a review. *Compr. Rev. Food Sci. Food Saf.* **2013**, *12* (1), 40–53.
- (29) Cui, H.; Zhao, C.; Lin, L. The specific antibacterial activity of liposome-encapsulated Clove oil and its application in tofu. *Food Control* **2015**, *56*, 128–134.
- (30) Jiang, P.; Li, D.; Xiao, Y.; Yang, X.; Liu, Y. Preparation and Characterization of Chitosan-Based Core–Shell Microcapsules Containing Clove Oil. *J. Nanosci. Nanotechnol.* **2015**, *15* (1), 600–605.
- (31) Cortés-Rojas, D. F.; Souza, C. R. F.; Oliveira, W. P. Encapsulation of eugenol rich clove extract in solid lipid carriers. *J. Food Eng.* **2014**, *127*, 34–42.
- (32) Kim, J. R.; Sharma, S. Acaricidal activities of clove bud oil and red thyme oil using microencapsulation against HDMs. *J. Microencapsulation* **2011**, *28* (1), 82–91.
- (33) Gao, K.; Liu, X. J.; Hao, X. L.; Liu, X. Preparation of Clove Essential Oil Microcapsule and Study on its Performance. *Appl. Mech. Mater.* **2014**, *651–653*, 269–272.
- (34) White, S. R.; Sottos, N. R.; Geubelle, P. H.; Moore, J. S.; Kessler, M. R.; Sriram, S. R.; Brown, E. N.; Viswanathan, S. Autonomic healing of polymer composites. *Nature* **2001**, *409* (6822), 794–797.
- (35) Samadzadeh, M.; Boura, S. H.; Peikari, M.; Kasirha, S. M.; Ashrafi, A. A review on self-healing coatings based on micro/nanocapsules. *Prog. Org. Coat.* **2010**, *68* (3), 159–164.
- (36) Cho, S. H.; Andersson, H. M.; White, S. R.; Sottos, N. R.; Braun, P. V. Polydimethylsiloxane-Based Self-Healing Materials. *Adv. Mater.* **2006**, *18* (8), 997–1000.
- (37) Wu, G.; An, J.; Tang, X.-Z.; Xiang, Y.; Yang, J. A Versatile Approach towards Multifunctional Robust Microcapsules with Tunable, Restorable, and Solvent-Proof Superhydrophobicity for Self-Healing and Self-Cleaning Coatings. *Adv. Funct. Mater.* **2014**, *24* (43), 6751–6761.
- (38) Yang, J.; Keller, M. W.; Moore, J. S.; White, S. R.; Sottos, N. R. Microencapsulation of Isocyanates for Self-Healing Polymers. *Macromolecules* **2008**, *41* (24), 9650–9655.
- (39) Huang, M.; Zhang, H.; Yang, J. Synthesis of organic silane microcapsules for self-healing corrosion resistant polymer coatings. *Corros. Sci.* **2012**, *65*, 561–566.
- (40) Zhang, H.; Yang, J. Development of self-healing polymers via amine–epoxy chemistry: I. Properties of healing agent carriers and the modelling of a two-part self-healing system. *Smart Mater. Struct.* **2014**, *23* (6), 065003.
- (41) Lee, H.; Choi, C.-H.; Abbaspourrad, A.; Wesner, C.; Caggioni, M.; Zhu, T.; Weitz, D. A. Encapsulation and Enhanced Retention of Fragrance in Polymer Microcapsules. *ACS Appl. Mater. Interfaces* **2016**, *8* (6), 4007–4013.
- (42) Subcommittee Standard Guide for Assessment of Antimicrobial Activity Using a Time-Kill Procedure; ASTM E2315-16; ASTM: West Conshohocken, PA, 2016.
- (43) Buckley, D. J.; Berger, M.; Poller, D. The swelling of polymer systems in solvents. I. Method for obtaining complete swelling–time curves. *J. Polym. Sci.* **1962**, *56* (163), 163–174.
- (44) Huang, M.; Yang, J. Facile microencapsulation of HDI for self-healing anticorrosion coatings. *J. Mater. Chem.* **2011**, *21* (30), 11123–11130.
- (45) Brown, E. N.; Kessler, M. R.; Sottos, N. R.; White, S. R. In situ poly(urea-formaldehyde) microencapsulation of dicyclopentadiene. *J. Microencapsulation* **2003**, *20* (6), 719–730.
- (46) Sun, D.; An, J.; Wu, G.; Yang, J. Double-layered reactive microcapsules with excellent thermal and non-polar solvent resistance for self-healing coatings. *J. Mater. Chem. A* **2015**, *3* (8), 4435–4444.
- (47) Varelas, C. G.; Dixon, D. G.; Steiner, C. A. Zero-order release from biphasic polymer hydrogels. *J. Controlled Release* **1995**, *34* (3), 185–192.
- (48) Korsmeyer, R. W.; Gurny, R.; Doelker, E.; Buri, P.; Peppas, N. A. Mechanisms of solute release from porous hydrophilic polymers. *Int. J. Pharm.* **1983**, *15* (1), 25–35.
- (49) Peppas, N. Analysis of Fickian and non-Fickian drug release from polymers. *Pharm. Acta Helv.* **1985**, *60*, 110–111.
- (50) Higuchi, T. Rate of release of medicaments from ointment bases containing drugs in suspension. *J. Pharm. Sci.* **1961**, *50* (10), 874–875.
- (51) Higuchi, T. Mechanism of sustained-action medication. Theoretical analysis of rate of release of solid drugs dispersed in solid matrices. *J. Pharm. Sci.* **1963**, *52* (12), 1145–1149.
- (52) Baker, R. W. *Controlled Release of Biologically Active Agents*; John Wiley & Sons, 1987.
- (53) Kanagasabhapathy, M.; Sasaki, H.; Haldar, S.; Yamasaki, S.; Nagata, S. Antibacterial activities of marine epibiotic bacteria isolated from brown algae of Japan. *Ann. Microbiol.* **2006**, *56* (2), 167.
- (54) Kimes, N. E.; Grim, C. J.; Johnson, W. R.; Hasan, N. A.; Tall, B. D.; Kothary, M. H.; Kiss, H.; Munk, A. C.; Tapia, R.; Green, L.; et al. Temperature regulation of virulence factors in the pathogen *Vibrio coralliilyticus*. *ISME J.* **2012**, *6* (4), 835–846.

- (55) Inbakandan, D.; Sriyutha Murthy, P.; Venkatesan, R.; Ajmal Khan, S. 16S rDNA sequence analysis of culturable marine biofilm forming bacteria from a ship's hull. *Biofouling* **2010**, *26* (8), 893–899.
- (56) López, M. A.; Díaz de la Serna, F. J. Z.; Jan-Roblero, J.; Romero, J. M.; Hernández-Rodríguez, C. Phylogenetic analysis of a biofilm bacterial population in a water pipeline in the Gulf of Mexico. *FEMS Microbiol. Ecol.* **2006**, *58* (1), 145–154.
- (57) Shikuma, N. J.; Hadfield, M. G. Marine biofilms on submerged surfaces are a reservoir for *Escherichia coli* and *Vibrio cholerae*. *Biofouling* **2010**, *26* (1), 39–46.
- (58) Walsh, S. E.; Maillard, J. Y.; Russell, A.; Catrenich, C.; Charbonneau, D.; Bartolo, R. Activity and mechanisms of action of selected biocidal agents on Gram-positive and-negative bacteria. *J. Appl. Microbiol.* **2003**, *94* (2), 240–247.
- (59) Oyedemi, S.; Okoh, A.; Mabinya, L.; Pirochenva, G.; Afolayan, A. The proposed mechanism of bactericidal action of eugenol, α -terpineol and g-terpinene against *Listeria monocytogenes*, *Streptococcus pyogenes*, *Proteus vulgaris* and *Escherichia coli*. *Afr. J. Biotechnol.* **2009**, *8*, (7).
- (60) Hemaiswarya, S.; Doble, M. Synergistic interaction of eugenol with antibiotics against Gram negative bacteria. *Phytomedicine* **2009**, *16* (11), 997–1005.
- (61) Gill, A.; Holley, R. Inhibition of membrane bound ATPases of *Escherichia coli* and *Listeria monocytogenes* by plant oil aromatics. *Int. J. Food Microbiol.* **2006**, *111* (2), 170–174.